Eur. Phys. J. D (2013)
DOI: 10.1140/epjd/e2013-30191-x

THE EUROPEAN PHYSICAL JOURNAL D

Regular Article

# Bessel beams of two-level atoms driven by a linearly polarized laser field

Armen G. Hayrapetyan[1,2,a], Oliver Matula[1,3], Andrey Surzhykov[4,5], and Stephan Fritzsche[4,5]

[1] Physikalisches Institut, Ruprecht-Karls-Universität Heidelberg, 69120 Heidelberg, Germany
[2] Max-Planck-Institut für Kernphysik, Postfach 103980, 69029 Heidelberg, Germany
[3] GSI Helmholtzzentrum für Schwerionenforschung, 64291 Darmstadt, Germany
[4] Helmholtz-Institut Jena, Fröbelstieg 3, 07743 Jena, Germany
[5] Theoretisch-Physikalisches Institut, Friedrich-Schiller-Universität Jena, Max-Wien-Platz 1, 07743 Jena, Germany

Received 20 March 2012 / Received in final form 8 April 2013
Published online (Inserted Later) – 

**Abstract.** We study Bessel beams of two-level atoms that are driven by a linearly polarized laser field. Starting from the Schrödinger equation, we determine the states of two-level atoms in a plane-wave field respecting propagation directions both of the atom and the field. For such laser-driven two-level atoms, we construct Bessel beams beyond the typical paraxial approximation. We show that the probability density of these atomic beams obtains a non-trivial, Bessel-squared-type behavior and can be tuned under the special choice of the atom and laser parameters, such as the nuclear charge, atom velocity, laser frequency, and propagation geometry of the atom and laser beams. Moreover, we spatially and temporally characterize the beam of hydrogen and selected (neutral) alkali-metal atoms that carry non-zero orbital angular momentum (OAM). The proposed spatiotemporal Bessel states (i) are able to describe, in principle, *twisted* states of any two-level system which is driven by the radiation field and (ii) have potential applications in atomic and nuclear processes as well as in quantum communication.

## 1 Introduction

The discovery of non-diffracting light fields by Durnin et al. [1,2] triggered an interest in studying Bessel beams of photons [3,4]. An intriguing property of these beams is that their intensity does not significantly change its shape over a propagation distance of a few centimeters [5,6]. The Bessel beams can also have several unusual features. For instance, they can carry a non-zero OAM and, thus, make their wavefronts rotate around the propagation axis while the Poynting vector draws a corkscrew, so called *twisted photons* [7,8]. The simplest object demonstrated to have such characteristics is the Laguerre-Gaussian beam as constructed in the seminal paper by Allen et al. [9]. Twisted photons, moreover, have led to recognizable advances in optical tweezers [10,11], atom trapping and guiding [12–15], transfer of OAM to a system of atoms [16,17], influence of OAM on beam shifts [18,19] and in other diverse applications [20–22].

In analogy with twisted photons, Bliokh et al. proposed a method to construct non-plane-wave solutions of the Schrödinger [23] and Dirac [24] equations for free electrons that exhibits non-zero OAM, called *twisted electrons*. These *vortex* beams of electrons have been produced experimentally for an energy of ∼200–300 keV only recently [25]. The electron vortex beams have found different applications as well, such as the magnetic mapping with atomic resolution in an electron microscope with twisted electrons [26,27] and improvement of electron microscopy of magnetic and biological specimens [28].

Although the photon and electron vortex beams have been quite extensively investigated, so far the first contribution in exploring the *atomic* Bessel beams, to the best of our knowledge, has been illustrated only in reference [29]. In an effort to extend the study of photon and electron vortex beams to other type of beams, we here demonstrate the construction of Bessel beams of *light* two-level atoms that are resonantly driven by the plane monochromatic laser beam.

In this work, we investigate Bessel beams of two-level atoms that are (resonantly) driven by a linearly polarized laser field. For these beams, we obtain solutions of the Schrödinger equation in terms of the *laser phase* by using an (invariant) approach as known from the relativistic theory [30]. We utilize these solutions in order to construct atomic *twisted* states that go beyond the typical paraxial approximation. Furthermore, we examine the spatial and temporal characteristics of the atomic Bessel beam *profile*. In particular, detailed calculations are performed especially for the probability density of hydrogen and light alkali-metal atom beams, that propagate perpendicular to the propagation direction of the laser beam. In this *crossed-beam* scenario, we show that the profile of atomic

[a] e-mail: armen@physi.uni-heidelberg.de

beams obtain a Bessel-squared-shape that is modified as the nuclear charge enlarges and can be tuned under the proper choice of laser parameters, such as the (resonant) frequency and the electric field strength. In addition, we also exhibit a possible enhancement of the second maximum in the profile of the potassium beam should the atom evolve in the field within a relatively long period, though in a time less than that of atomic decay.

The paper is organized as follows. In the next section, we define the twisted states of a freely moving atom and describe their main properties. In order to see how the laser beam influences the Bessel-squared-type distribution of the atomic beam profile, in Section 3.1, we define the classical laser field and the geometry of the laser and atomic beams propagation, namely the collinear- and crossed-beam scenarios. For the interaction of a two-level atom with a linearly polarized monochromatic plane-wave field, equations are then derived for the atomic probability amplitudes within the center-of-mass frame of the atom. *Exact* analytical solutions to these equations are found within the eikonal (EA), the long-wave (LWA) and the rotating-wave (RWA) approximations. These solutions are then utilized in Section 3.2 in order to construct the twisted states of laser-driven two-level atoms in both, collinear- and crossed-beam scenarios. In Section 4, we analyze the probability density of these (Bessel) beams of hydrogen and selected alkali-metal atoms, such as Li, Na and K, when (resonantly) driven on the $1s \leftrightarrow 2p$, $2s \leftrightarrow 2p$, $3s \leftrightarrow 3p$ and $4s \leftrightarrow 4p$ atomic transitions, respectively. In particular, we display and discuss the spatiotemporal characteristics of these beams in the crossed-beam scenario. Finally, a few conclusions and proposals are drawn in Section 5 and a detailed derivation of the solution to the Schrödinger equation (with respecting propagation directions both of the atomic and the laser beams) is illustrated in 5.

## 2 Twisted states of free atoms

A Bessel beam of any quantum particle is defined as a (*twisted*) state with its well defined energy $\mathcal{E}_0$, longitudinal momentum $p_{||0}$, absolute value of the transverse momentum $p_{\perp 0}$ as well as the projection $\hbar\ell$ of the OAM on the propagation axis [7,8,24,31,32]. In accordance to this definition, the spectrum of such states can be represented in the form

$$\tilde{\psi}_\ell(\boldsymbol{p}) = \delta(\mathcal{E}-\mathcal{E}_0)\delta(p_\perp - p_{\perp 0})\,\delta(p_{||}-p_{||0})\frac{e^{i\ell\phi}}{2\pi i^\ell p_{\perp 0}} \quad (1)$$

that contains a vortex phase dependency $e^{i\ell\phi}$, and where $\ell$ is an integer. Such spectrum means that the momentum of the atom is distributed over some cone with slant length $p_0 = \sqrt{p_{||0}^2 + p_{\perp 0}^2} = \text{const.}$ and fixed polar angle $\theta_0$ with regard to the $z$-axis (cf. Fig. 1, the blue sketch). The 'size' of this cone is defined such as the longitudinal and transverse components of the beam momentum are equal to $p_{||0} = p_0\cos\theta_0$ and $p_{\perp 0} = p_0\sin\theta_0$,

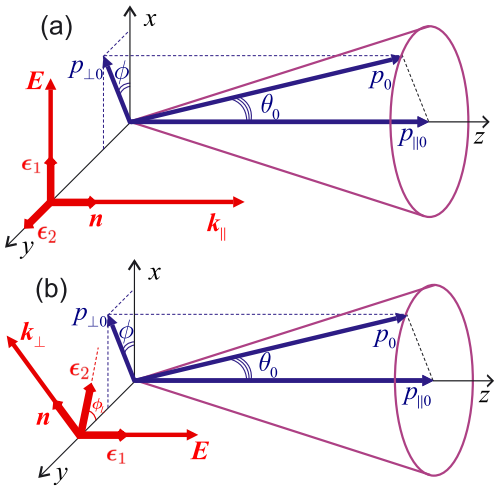


**Fig. 1.** Collinear-beam (a) and crossed-beam (b) scenarios for the interposition of linearly polarized laser and atomic Bessel beams. Red sketches indicate directions of the field polarization and the wave vector. Blue sketches indicate the momentum distribution of the atomic Bessel beam. A twisted two-level atom driven by the laser field is a superposition of the orthonormalized waves (18) (a) or (20) (b) with a fixed conical momentum spread $p_0 = \text{const.}$, polar angle $\theta_0$ and the azimuthal phase factor $e^{i\ell\phi}$.

respectively. Owing to the conical symmetry of the momentum distribution, we shall use cylindrical coordinates $\boldsymbol{p} = (p_\perp, \phi, p_{||}) = (p\sin\theta, \phi, p\cos\theta)$ in momentum space and construct a Bessel-type solution of the Schrödinger (free wave) equation

$$\psi_\ell(\boldsymbol{r},t) = \int \tilde{\psi}_\ell(\boldsymbol{p})\;\psi^{PW}(\boldsymbol{r},t)\,p_\perp dp_\perp d\phi\, dp_{||} \quad (2)$$

as a superposition of plane waves

$$\psi^{PW}(\boldsymbol{r},t) = e^{\frac{i}{\hbar}(\boldsymbol{p}\cdot\boldsymbol{r}-\mathcal{E}t)} \quad (3)$$

over the spectrum (1) of such a cone.

Integration (2) can be readily performed if we take into account the cylindrical symmetry of the atomic beam propagation and use the cylindrical coordinates in the position space as well, $\boldsymbol{r} = (r,\varphi,z)$. These coordinates, along with the cylindrical coordinates in momentum space, enable one to re-write the scalar product as

$$\boldsymbol{p}\cdot\boldsymbol{r} = p_\perp r\cos(\phi-\varphi) + p_{||}z$$

in the plane wave (3) and, therefore, to exploit the integral representation

$$\int_0^{2\pi} d\phi\, e^{i\ell\phi}e^{i\xi\cos(\phi-\varphi)} = 2\pi i^\ell e^{i\ell\varphi}J_\ell(\xi) \quad (4)$$

of the Bessel function [33]. Direct integration simply leads to the final form of the twisted state of a free atom

$$\psi_\ell(\boldsymbol{r},t) = e^{\frac{i}{\hbar}(p_{||0}z-\mathcal{E}_0 t)}e^{i\ell\varphi}J_\ell(\xi), \quad (5)$$

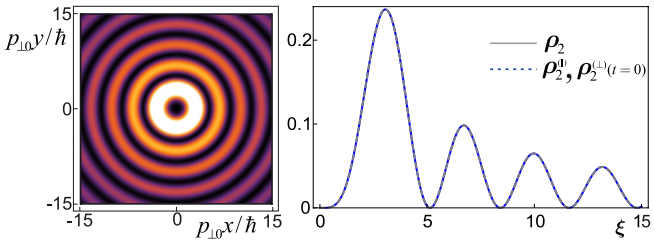


**Fig. 2.** Distribution of probability density (in arbitrary units) over the dimensionless transverse coordinate for free (gray solid curve) and laser-driven (blue dashed curve) beams of twisted atoms with OAM $\hbar\ell = 2\hbar$. For the crossed-beam scenario, the probability density $\rho_2^{(\perp)}$ is depicted at $t = 0$ when the field is switched off. The distribution is shown by the variation of colors from black to white within the 'sunset' scale (left panel), where black and white correspond to the minimum and maximum values of the probability density.

where $\xi = p_{\perp 0} r/\hbar$ is a dimensionless transverse coordinate which characterizes the *width* of the beam. As seen from equation (5), the state $\psi_\ell(\boldsymbol{r}, t)$ represents an atomic beam that propagates freely along the $z$-direction, $e^{ip_{||0}z/\hbar}$, and has the profile

$$\rho_\ell \equiv |\psi_\ell(\boldsymbol{r}, t)|^2 = J_\ell^2(\xi), \tag{6}$$

a Bessel-squared-shape in the radial dimension (as also illustrated in Fig. 2). The vortex phase factor $e^{i\ell\varphi}$ ensures that the twisted state (5) is an eigenstate of the $z$-component of OAM operator $\hat{\ell}_z = -i\hbar\partial/\partial\varphi$, and, thus, is responsible for non-zero OAM $\hbar\ell$ on the propagation axis. In addition, one should stress that the states (5) are orthogonal and can be normalized if the integration is carried out, for instance, over a large, but finite cylindrical volume. For our further analysis, however, the normalization is not of crucial interest.

We have shown a simple, but very significant procedure how one can create twisted states of a free particle (e.g. atom). In our later study, we are interested in how these twisted states are affected by an external influence, such as a driving laser field. For this purpose, we will initially prepare a two-level atom in the upper state and then *switch on* the laser field. Once this atom is coherently driven by the field, we will apply the same approach in order to construct Bessel beams of such atoms and to investigate their spatiotemporal characteristics.

## 3 Twisted states of laser-driven atoms

In the previous section, we have shown a simple way of construction of free atomic Bessel beams. In this section, we are interested in the dynamics of these beams when they are (coherently) driven by the field of a plane monochromatic laser wave. To this end, in Section 3.1, we examine the coherent coupling of a two-level atom with the linearly polarized radiation field, and then, in Section 3.2, we construct the twisted states of this laser-driven atom by employing the (Bessel) spectrum (1).

### 3.1 Semi-classical coupling of two-level atoms to a laser field

The coherent interaction of a two-level atom with the radiation field has been explored since the early days of quantum optics [34–37]. Nowadays, this *atomic coherence* is known as an effective tool for achieving control about (atomic and molecular) samples [38–40] and it can be utilized to examine various effects with atomic beams, such as generation of entanglement [41], investigation of the optical force [42,43] or exhibition of vortices [44–46] in beams. In order to examine how this coherent control can be exploited *also* for tuning and guiding the atomic Bessel beams, in the following, we shall describe the coherent coupling of an atom to the laser field in the meantime respecting the propagation directions of both the atom and laser beams.

To describe the interaction of a two-level atom with a *classical* radiation field and to start our derivations, let us first characterize the field and the interaction (Hamiltonian) between the atom and this field. We hereby assume that the atom has the (rest) mass $m$, a dipole moment $\boldsymbol{d}$, and that it moves with constant momentum $\boldsymbol{p}$ along some *given* direction.

#### 3.1.1 Characterization of the classical field

We consider the classical electric field of laser beam as a (monochromatic) plane wave

$$\boldsymbol{E} = \boldsymbol{\varepsilon}\, e^{i(\boldsymbol{k}\cdot\boldsymbol{r}-\omega t)}, \tag{7}$$

with constant electric-field amplitude $\boldsymbol{\varepsilon}$, frequency $\omega$ and wave vector $\boldsymbol{k} \equiv k\,\boldsymbol{n}$, which satisfies Maxwell's equations, and where the unit vector $\boldsymbol{n}$ defines the propagation direction of the wave [47]. While, in general, $\boldsymbol{E}$ and $\boldsymbol{\varepsilon}$ are both complex-valued vectors in equation (7), the physically relevant *electric* field is given by the real part, $\Re(\boldsymbol{E})$, and is for transverse waves always perpendicular to its propagation, i.e. $\boldsymbol{n}\cdot\boldsymbol{\varepsilon} = 0$. For our further discussion, moreover, it is useful to introduce a set of real and mutually orthogonal unit vectors $(\boldsymbol{\epsilon}_1, \boldsymbol{\epsilon}_2, \boldsymbol{n})$, and to re-write the field amplitude in terms of these vectors as

$$\boldsymbol{\varepsilon} = \boldsymbol{\epsilon}_1\,\varepsilon_0 + \boldsymbol{\epsilon}_2\,\varepsilon_0', \tag{8}$$

with the two (complex) constants $\varepsilon_0$ and $\varepsilon_0'$.

Most generally, the laser field amplitude $\boldsymbol{\varepsilon}$ in equation (7) describes an *elliptically* polarized plane wave; as a special case, this definition includes *linearly* polarized waves if the complex constants $\varepsilon_0$ and $\varepsilon_0'$ fulfill proper relations. We choose $\varepsilon_0' = 0$ which corresponds to a linearly polarized field in $\boldsymbol{\epsilon}_1$ direction

$$\boldsymbol{E}(\boldsymbol{r}, t) = \boldsymbol{\epsilon}_1\,\varepsilon_0\, e^{i(\boldsymbol{k}\cdot\boldsymbol{r}-\omega t)}$$

with the (real) amplitude $\varepsilon_0$. Therefore, for this wave the relevant electric field is given by

$$\boldsymbol{E} = \boldsymbol{\epsilon}_1\varepsilon_0\cos\zeta = \boldsymbol{\varepsilon}\cos\zeta, \tag{9}$$

where $\zeta \equiv \boldsymbol{k}\cdot\boldsymbol{r}-\omega t$ is the *phase* of the plane wave independent of its particular polarization properties. We here should stress that the field is evaluated at the center-of-mass position $\boldsymbol{r}\equiv(x,y,z)$ of the atom.

The field and the atom propagation directions, in principle, can be chosen arbitrarily which will form the geometry of the "atom + laser" system. To describe the linearly polarized laser field we specify this geometry already in this subsection. We examine two scenarios that depend on the interposition of the propagation directions of laser and atomic beams. These are the so-called *collinear-* and *crossed-beam* scenarios for which the laser and the atomic beam propagation directions correspondingly are parallel or perpendicular to each other (cf. Fig. 1). As mentioned above, the $z$-axis is chosen along the propagation direction of the atomic beam. In collinear-beam scenario, moreover, we chose the $x$- and $z$-axes directed along the polarization $\boldsymbol{\epsilon}_1$ and laser beam propagation, respectively. In contrast to this, in crossed-beam scenario, we restrict ourselves with the polarization along $z$-axis and consider propagation in $x$-$y$-plane, where the $x$-axis is declined from the laser propagation direction under $\phi_L$ angle.

With the distinction of these collinear- and crossed-beam scenarios the laser field (9) and the phase $\zeta$ obtain the form

$$\boldsymbol{E}^{(||)}=(\varepsilon\cos\zeta^{(||)},0,0)\,,\ \zeta^{(||)}=k_{||}z-\omega t, \tag{10}$$

$$\boldsymbol{E}^{(\perp)}=(0,0,\varepsilon\cos\zeta^{(\perp)})\,,\ \zeta^{(\perp)}=k_{\perp}r\cos(\phi_L-\varphi)-\omega t, \tag{11}$$

respectively, with a transverse coordinate $r\equiv\sqrt{x^2+y^2}$ of the atomic center-of-mass. In the following, we define the Hamiltonian of our system and determine the atomic states that are driven by the laser field (10) and (11).

### 3.1.2 Solution of the Schrödinger equation in the center-of-mass frame of the atom

In the semi-classical theory, the quantum dynamics of the atom is driven by the external field but this "motion" does *not* re-act back upon the field as this would require a quantization of the electromagnetic field [34]. Therefore, the Hamiltonian of an atom in the (classical) field takes the form

$$H=\frac{\hat{p}^2}{2m}+H_{\rm atom}+H_{\rm int}, \tag{12}$$

where $\frac{\hat{p}^2}{2m}$ denotes the kinetic energy (operator) as associated with the center-of-mass motion and

$$H_{\rm atom}=E_a\left|a\right\rangle\left\langle a\right|+E_b\left|b\right\rangle\left\langle b\right| \tag{13}$$

refers to the internal motion of the atom, whilst the interaction of the atom and the field is taken (as usual) in *minimal* coupling

$$H_{\rm int}=-\boldsymbol{d}\cdot\boldsymbol{E}$$

in the LWA [37]. The two state vectors $|a\rangle$ and $|b\rangle$ in expression (13) denote the upper and lower states of the atom and are supposed to be eigenstates of the atomic Hamiltonian

$$H_{\rm atom}\left|a\right\rangle=E_a\left|a\right\rangle$$
$$H_{\rm atom}\left|b\right\rangle=E_b\left|b\right\rangle,$$

and where $E_a$ and $E_b$ are the energies of upper and lower states, respectively.

Making use of the completeness $\left|a\right\rangle\left\langle a\right|+\left|b\right\rangle\left\langle b\right|=1$ for a two-level system, the interaction Hamiltonian of the atom with a linearly-polarized wave can be written in the form

$$H_{int}^{(||)}=-\hbar\Omega_{R_x}\big(e^{i\phi_{d_x}}\left|b\right\rangle\left\langle a\right|+e^{-i\phi_{d_x}}\left|a\right\rangle\left\langle b\right|\big)\cos\zeta^{(||)}, \tag{14}$$

$$H_{int}^{(\perp)}=-\hbar\Omega_{R_z}\big(e^{i\phi_{d_z}}\left|b\right\rangle\left\langle a\right|+e^{-i\phi_{d_z}}\left|a\right\rangle\left\langle b\right|\big)\cos\zeta^{(\perp)} \tag{15}$$

for collinear- and crossed-beam scenarios, respectively. In accordance to these scenarios, here $\Omega_{R_x}=\left|e\left\langle b\right|\tilde{x}\left|a\right\rangle\right|\varepsilon_0/\hbar$ and $\Omega_{R_z}=\left|e\left\langle b\right|\tilde{z}\left|a\right\rangle\right|\varepsilon_0/\hbar$ denote the Rabi frequencies that describe the coupling strength of the atom either with the $x$- (10) or $z$-polarized (11) field, respectively. With this distinction for the Rabi frequencies, the exponentials $\phi_{d_x}$ and $\phi_{d_z}$ denote the phases of the dipole matrix elements: $e\left\langle b\right|u\left|a\right\rangle=\left|e\left\langle b\right|u\left|a\right\rangle\right|e^{i\phi_{d_u}}$ where $u=\tilde{x},\tilde{z}$. Here both $\tilde{x}$ and $\tilde{z}$ refer to so-called internal variables of the atom and are the electron's relative coordinates with regard to the nucleus [37]. The Rabi frequencies, moreover, arise naturally as non-diagonal matrix elements of the atom dipole moment if we express the interaction Hamiltonian in the $\{|a\rangle,|b\rangle\}$ basis. This, in turn, makes the interaction Hamiltonian dependent on atomic states $|a\rangle$, $|b\rangle$ and the center-of-mass coordinate of the atom[1].

For such an effective factorization of the interaction Hamiltonian, and as described in many texts before [34–36], the two-level atom undergoes Rabi oscillations between its lower and upper states with frequency $\Omega_{R_x}$ or $\Omega_{R_z}$, quite analogue to a spin-1/2 system in an oscillating magnetic field [48]. In contrast to the standard derivation (see, for example, Ref. [34]), however, the interaction Hamiltonian (14)–(15) now also depends on the phase $\zeta^{(||)}$ and $\zeta^{(\perp)}$ of the radiation field to account for the time- *and* space-dependency of the atom-laser interaction. In addition, some time ago an approximate technique, i.e. expansion of the exponent (7) in the interaction Hamiltonian, has been applied to the helium and hydrogen atoms in order to examine their coupling to an intense laser field [49].

To explore the time evolution of the atom, let us search for solutions of the (time-dependent) Schrödinger equation

$$H\psi=i\hbar\frac{\partial\psi}{\partial t}. \tag{16}$$

[1] Hereinafter, for notational convenience we drop the "tilde" of the indexes $x$ and $y$ at the Rabi frequencies and the exponentials of the dipole matrix elements. This will not cause a confusion since already at this step the dependence on the electron's relative coordinate is eliminated in the interaction Hamiltonian (14)–(15).

If we utilize the (effective) factorization of the interaction Hamiltonian we can use the ansatz

$$\psi\left(\boldsymbol{r},t\right)=e^{\frac{i}{\hbar}\left(\boldsymbol{p}\cdot\boldsymbol{r}-\mathcal{E}t\right)}\left(\psi_a(\zeta)\ |a\rangle+\psi_b(\zeta)\ |b\rangle\right), \quad (17)$$

as a solution of the Schrödinger equation. Here $\zeta\equiv\zeta^{(||)}$, $\zeta^{(\perp)}$ is the laser phase for collinear- or crossed-beam scenarios, respectively. The constant (non-relativistic) momentum $\boldsymbol{p}\equiv m\boldsymbol{v}$ of the center-of-mass of atom gives hereby rise to the space-dependent "translation factor" $e^{\frac{i}{\hbar}\boldsymbol{p}\cdot\boldsymbol{r}}$ to account for its overall motion with energy $\mathcal{E}$ within the given coordinates. A similar ansatz has been applied in reference [50] in order to investigate Stark splitting of a three-level atom.

We give the detailed derivation of the solution of the Schrödinger equation (16) in 5 where the physical assumptions we consider are the following. We prepare the atom initially in the upper state (cf. Eq. (A.16)) and then employ the typical, *eikonal* and *rotating wave* approximations, for which the atom rest energy is much larger than the photon energy (EA) that, in turn, is resonant to the atomic transition energy (RWA, see also Eq. (A.17)). For light two-level atoms, both the EA and RWA are valid with high accuracy [34]. Under these physically relevant conditions, we obtain analytically exact solution

$$\psi^{(||)}\left(\boldsymbol{r},t\right)=e^{\frac{i}{\hbar}\left(\boldsymbol{p}\cdot\boldsymbol{r}-\mathcal{E}t\right)}\left(e^{-i\alpha^{(||)}\zeta^{(||)}}\cos\frac{\Omega^{(||)}\zeta^{(||)}}{2}\,|a\rangle+ie^{i\phi_{d_x}}e^{-i\beta^{(||)}\zeta^{(||)}}\sin\frac{\Omega^{(||)}\zeta^{(||)}}{2}\,|b\rangle\right) \quad (18)$$

that represents the state of the laser-driven two-level atom for collinear-beam scenario with some reduced quantities (cf. Eq. (A.3))

$$\{\alpha^{(||)},\,\beta^{(||)},\,\Omega^{(||)}\}\equiv\frac{\{E_a,\,E_b,\,\Omega_{R_x}\}}{\hbar\left(kv_{||}-\omega\right)}. \quad (19)$$

Whereas, in crossed-beam scenario, the atomic state is given by

$$\psi^{(\perp)}\left(\boldsymbol{r},t\right)=e^{\frac{i}{\hbar}\left(\boldsymbol{p}\boldsymbol{r}-\mathcal{E}t\right)}\left(e^{-i\alpha^{(\perp)}\zeta^{(\perp)}}\cos\frac{\Omega^{(\perp)}\zeta^{(\perp)}}{2}\,|a\rangle+ie^{i\phi_{d_z}}e^{-i\beta^{(\perp)}\zeta^{(\perp)}}\sin\frac{\Omega^{(\perp)}\zeta^{(\perp)}}{2}\,|b\rangle\right) \quad (20)$$

with reduced quantities

$$\hbar\,\{\alpha^{(\perp)},\,\beta^{(\perp)},\,\Omega^{(\perp)}\}\equiv\frac{\{E_a,\,E_b,\,\Omega_{R_z}\}}{kv_\perp\cos(\phi_L-\phi)-\omega}. \quad (21)$$

In equations (18)–(21), $p^2=p_{||}^2+p_\perp^2$ is the squared total momentum of the atom (with its longitudinal $p_{||}$ and transverse $p_\perp$ components and the atomic velocities $v_{||}=p_{||}/m$ and $v_\perp=p_\perp/m$, respectively). The *orthonormalized* solutions (18) and (20) represent a superposition of the upper $|a\rangle$ and lower $|b\rangle$ states with $\zeta^{(||)}$- or $\zeta^{(\perp)}$-dependent coefficients. The 'translation' factor $e^{\frac{i}{\hbar}\left(\boldsymbol{p}\cdot\boldsymbol{r}-\mathcal{E}t\right)}$, as mentioned above, describes the motion of the atom as a whole with momentum vector $\boldsymbol{p}$ along some (chosen) direction and energy $\mathcal{E}$.

So far, the focus of this subsection was placed on determining solutions of the Schrödinger equation (16) for linearly polarized field (10) or (11). In the next subsection, we will utilize the *explicit* $\boldsymbol{r}$-dependency of (exact) solutions (18) and (20) and exploit them in order to construct a *Bessel beam* of laser-driven two-level atoms.

## 3.2 Twisted states of laser-driven two-level atoms

In the previous subsection, we have analyzed the time- and space-dependent interaction of two-level atoms with a linearly polarized laser field and have built the states (18) and (20) which describe the *spatiotemporal* dynamics of laser-driven atoms. In the following, we shall utilize these states in order to construct atomic Bessel beams which carry a non-zero OAM and meanwhile do not diffract along the propagation direction.

The wave function of the laser-driven two-level atom with the projection $\hbar\ell$ of the OAM on the (atomic beam) propagation axis can be constructed as a superposition of orthonormalized solutions (18) and (20) of the time-dependent Schrödinger equation (16)

$$\Psi_\ell\left(\boldsymbol{r},t\right)=\int\tilde{\psi}_\ell\left(\boldsymbol{p}\right)\,\psi\left(\boldsymbol{r},t\right)p_\perp dp_\perp d\phi\,dp_{||} \quad (22)$$

over the *monoenergetic* cone (1). This step in the construction of *twisted* atomic beams is analogue to the use of twisted photons [7,8] and electrons [24].

### 3.2.1 Collinear-beam scenario

Let us start with the collinear-beam scenario for which the integration (22) can be carried out easily in a similar way as for the twisted state (5) of a free atom. Indeed, by performing the same steps, i.e. substituting the state (18) into equation (22) and making use of the integral representation (4) of Bessel function, we obtain a *simple* form for the twisted state of a laser-driven two-level atom

$$\Psi_\ell^{(||)}=e^{\frac{i}{\hbar}\left(p_{||0}z-\mathcal{E}_0t\right)}e^{i\ell\varphi}J_\ell\left(\xi\right)\left(e^{-i\alpha_0^{(||)}\zeta^{(||)}}\cos\frac{\Omega_0^{(||)}\zeta^{(||)}}{2}\,|a\rangle+ie^{i\phi_{d_x}}e^{-i\beta_0^{(||)}\zeta^{(||)}}\sin\frac{\Omega_0^{(||)}\zeta^{(||)}}{2}\,|b\rangle\right). \quad (23)$$

Here the dimensionless transverse coordinate $\xi=p_{\perp0}r/\hbar$ describes the width of the beam, and the reduced quantities $\alpha_0^{(||)}$, $\beta_0^{(||)}$ and $\Omega_0^{(||)}$ are taken on the cone 'surface' $p=p_0$ (cf. Eq. (19) and Fig. 1a).

The state (23) is the eigenstate of the $z$-component of OAM operator $\hat{\ell}_z$ due to the presence of the vortex phase factor $e^{i\ell\varphi}$. Hence, apart from the free propagation along the $z$-direction, $e^{ip_{||0}z/\hbar}$, and the Bessel-dependency on the (dimensionless) transverse coordinate the twisted state $\Psi_\ell^{(||)}$ also carries a well-defined OAM $\hbar\ell$ quite similar to the scalar [23,51] and spin-dependent [24] electron Bessel beams.

It is obvious that when the field is switched off, i.e. $\Omega_0^{(||)} = \zeta^{(||)} = 0$, the free twisted state (5) is recovered. The presence of the field causes only Rabi flopping of (already) twisted two-level atoms between the upper $|a\rangle$ and lower $|b\rangle$ states and meantime does *not* influence the Bessel-squared-shape of the beam profile. Alluding to Section 4, let us note that the absence of the field's impact on the beam profile is quite expected since the laser phase $\zeta^{(||)} = k_{||}z - \omega t$ in collinear-beam scenario contributes only in the free motion of the atomic beam along the $z$-axis and does not contain the radial coordinate $r$ in contrast to the laser phase $\zeta^{(\perp)}$ in crossed-beam scenario where both $r$ and the azimuthal angle $\varphi$ are involved (cf. Eqs. (10)–(11)). It is the presence of $r$ and $\varphi$ that enables one to explore an intriguing dynamics of atomic twisted states in crossed-beam scenario as we exhibit in details in our forthcoming discussion.

### 3.2.2 Crossed-beam scenario

So far, we have investigated the twisted states of free (5) and of laser-driven atoms in the collinear-beam scenario (23). These two states involve the same, *stationary* Bessel-dependency $J_\ell(\xi)$ in the profile of the beam. Whereas, the crossed-beam scenario gives rise to a time-dependent atomic beam profile. To investigate this we shall evaluate the integral (22) by employing the solution (20). This integration cannot be carried out by means of exact methods since the reduced quantities $\alpha^{(\perp)}$, $\beta^{(\perp)}$ and $\Omega^{(\perp)}$ depend on the $\phi$ angle (compare Eqs. (19) and (21)). However, if we consider a *non-relativistic regime* for the propagation of atomic beam we can easily proceed analytically. For this purpose, we again represent the scalar product in the form $\boldsymbol{p}\cdot\boldsymbol{r} = p_\perp r\cos(\phi-\varphi) + p_{||}z$ and evaluate the integral (22) first with respect to transverse $p_\perp$ and longitudinal $p_{||}$ components of the (linear) momentum

$$\Psi_\ell^{(\perp)} = \frac{e^{\frac{i}{\hbar}(p_{||0}z-\mathcal{E}_0 t)}}{4\pi i^\ell} \times \int_0^{2\pi} d\phi\, e^{i\ell\phi} e^{i\xi\cos(\phi-\varphi)} \sum_{n=1}^{4} e^{i\mathcal{A}_n\zeta^{(\perp)}} |\mathcal{B}_n\rangle\,, \quad (24)$$

where the state vectors

$$|\mathcal{B}_{1,2}\rangle \equiv |a\rangle\,,\ |\mathcal{B}_{3,4}\rangle \equiv \pm e^{i\phi_{dz}}\,|b\rangle$$

refer to the upper and lower levels of the atom. For the sake of brevity, moreover, we introduce the dimensionless parameters

$$\mathcal{A}_{1,2} \equiv -\alpha_0^{(\perp)} \pm \Omega_0^{(\perp)}/2,\ \mathcal{A}_{3,4} \equiv -\beta_0^{(\perp)} \pm \Omega_0^{(\perp)}/2, \quad (25)$$

which carry information about the internal structure of the atom and the strength of the atom-field coupling. These parameters are given in terms of the reduced quantities $\alpha_0^{(\perp)}$, $\beta_0^{(\perp)}$ and $\Omega_0^{(\perp)}$ and are taken at the cone surface $p = p_0$.

Now we apply our assumption about the non-relativistic regime for the propagation of atomic beam and Taylor expand $\mathcal{A}_n$ $(n = 1\ldots 4)$ by keeping only the terms up to the first power in $v_{\perp 0}/c$

$$\mathcal{A}_n \approx \mathcal{C}_n\left(1 + \frac{v_{\perp 0}}{c}\cos(\phi_L - \phi)\right),$$

where

$$\mathcal{C}_{1,2} \equiv (E_a \mp \hbar\Omega_{R_z}/2)/(\hbar\omega),\ \mathcal{C}_{3,4} \equiv (E_b \mp \hbar\Omega_{R_z}/2)/(\hbar\omega)$$

are dimensionless constant energies normalized to the photon energy. This expansion enables one to re-write the wave function (24) in a desired form

$$\Psi_\ell^{(\perp)} = \frac{e^{\frac{i}{\hbar}(p_{||0}z-\mathcal{E}_0 t)}}{4\pi i^\ell} \times \sum_{n=1}^{4} e^{i\mathcal{C}_n\zeta^{(\perp)}} \int_0^{2\pi} d\phi\, e^{i\ell\phi} e^{i\mathcal{X}_n\cos\phi} e^{i\mathcal{Y}_n\sin\phi}\,|\mathcal{B}_n\rangle \quad (26)$$

which is appropriate for analytical integration. Here, the dimensionless *coordinates*

$$\mathcal{X}_n(\xi,\varphi,t) \equiv \xi\cos\varphi + \mathcal{C}_n\zeta^{(\perp)}\frac{v_{\perp 0}}{c}\cos\phi_L,$$
$$\mathcal{Y}_n(\xi,\varphi,t) \equiv \xi\sin\varphi + \mathcal{C}_n\zeta^{(\perp)}\frac{v_{\perp 0}}{c}\sin\phi_L \quad (27)$$

contain the (time-dependent) laser phase

$$\zeta^{(\perp)} = \frac{\hbar k}{p_{\perp 0}}\xi\cos(\phi_L - \varphi) - \omega t, \quad k \equiv k_\perp \quad (28)$$

that is independent of the integration variable $\phi$.

In order to calculate the integral (26) we introduce a new system of "cartesian" $\boldsymbol{R}_n \equiv (\mathcal{X}_n, \mathcal{Y}_n, \mathcal{Z})$ and "cylindrical" $\boldsymbol{R}_n \equiv (\Xi_n, \Phi_n, \mathcal{Z})$ coordinates with standard transformations

$$\mathcal{X}_n = \Xi_n\cos\Phi_n, \quad \mathcal{Y}_n = \Xi_n\sin\Phi_n, \quad \mathcal{Z} = p_{\perp 0}z/\hbar, \quad (29)$$

where $\Xi_n = \sqrt{\mathcal{X}_n^2 + \mathcal{Y}_n^2}$ is the "radial" coordinate and $\Phi_n$ is the "azimuthal angle" in the $(\mathcal{X}_n, \mathcal{Y}_n)$-plane. By inserting these new coordinates in equation (26) and making use of a simple trigonometric relation, we can exploit the integral representation of the Bessel function

$$\int_0^{2\pi} d\phi\, e^{i\ell\phi} e^{i\Xi_n\cos(\phi-\Phi_n)} = 2\pi i^\ell e^{i\ell\Phi_n} J_\ell(\Xi_n)$$

and obtain the final form of the twisted state of laser-driven two-level atoms in crossed-beam scenario

$$\Psi_\ell^{(\perp)} = \frac{1}{2} e^{\frac{i}{\hbar}(p_{||0}z-\mathcal{E}_0 t)} \sum_{n=1}^{4} e^{i\mathcal{C}_n\zeta^{(\perp)}} e^{i\ell\Phi_n} J_\ell(\Xi_n)\,|\mathcal{B}_n\rangle. \quad (30)$$

It is important to note that we recover the free twisted state (5) if we switch off the laser field (i.e. $\zeta^{(\perp)} \to 0$), since in this case the coordinates $\Xi_n$ and $\Phi_n$ coincide with $\xi$ and $\varphi$, respectively, as $(\mathcal{X}_n, \mathcal{Y}_n) \to (p_{\perp 0}x/\hbar, p_{\perp 0}y/\hbar)$ (cf. Eq. (27)).

Since no restriction has been made on the longitudinal $p_{||0}$ and transverse components $p_{\perp 0}$ of the atom momentum, the states (23) and (30) apply generally for scalar Bessel beams of two-level atoms *beyond* the typical paraxial approximation for both, the collinear- and crossed-beam scenarios. As we stressed above, we are not interested in the normalization of these states since it does not provide too much insight in the overall dynamics of the beam. To give a hint, however, we would like to point out that these beams, can be normalized, on one hand, by integrating them in a large, but a finite cylindrical volume, as already mentioned above and also done in references [31,32] for twisted photons. On the other hand, we could regularize the Dirac $\delta$-function, which arises after the integration of squared Bessel functions over the whole space, by rigorously re-defining it as a limit of regular functions (e.g. Gaussian), as also mentioned in reference [24] for electron Bessel beams.

In the last discussion of this section, we put the emphasis on finding an integral of "motion" that describes the propagation of the laser-driven twisted atom in the crossed-beam scenario. A similar operator description of angular momentum properties of light Bessel beams has been done in reference [52]. Given that the photon energy and momentum are much less than the atom rest energy and transverse momentum, respectively, i.e. $\hbar\omega/(mc^2) \ll 1$ and $\hbar k/(mv_{\perp 0}) \ll 1$, we replace (27) with the following approximate relations

$$\begin{aligned} \mathcal{X}_n &\approx \xi\cos\varphi - \mathcal{C}_n v_{\perp 0} kt\cos\phi_L, \\ \mathcal{Y}_n &\approx \xi\sin\varphi - \mathcal{C}_n v_{\perp 0} kt\sin\phi_L, \end{aligned} \tag{31}$$

that are valid with high accuracy for a wide range of frequencies, from infrared to ultraviolet regions. The wave function (30), therefore, can be re-written as

$$\Psi_\ell^{(\perp)} \approx \sum_{n=1}^{4} \Psi_\ell^{(n)}, \tag{32}$$

$$\Psi_\ell^{(n)} \equiv \frac{1}{2} e^{\frac{i}{\hbar}(p_{||0}z - (\mathcal{E}_0 + \mathcal{C}_n\hbar\omega)t)} e^{i\ell\Phi_n} J_\ell(\Xi_n)\,|\mathcal{B}_n\rangle\,, \tag{33}$$

where we have replaced the laser phase (28) with $\zeta^{(\perp)} \approx -\omega t$. One can immediately recognize that the exponential $e^{ip_{||0}z/\hbar}$ describes the diffraction-free propagation of the beam along the $z$-axis. Moreover, this free propagation occurs as a sum of four scalar Bessel modes $\Psi_\ell^{(n)}$, each of which carries a quasi-energy $\mathcal{E}_0 + \mathcal{C}_n\hbar\omega$ because the atom is dressed by the field.

The notable difference between the twisted states of laser-driven (also of free) atoms in collinear- and crossed-beam scenarios is that here the Bessel function depends on the new coordinate $\Xi_n$ and, consequently, on time (compare Eqs. (23) and (5) with Eq. (32)). Due to this (different) dependency, the state (32) is no longer the eigenstate of the *conventional* OAM operator $\hat{\ell}_z = -i\hbar\partial/\partial\varphi$, instead each of the modes (33) represents an eigenstate of the operator

$$\hat{\mathcal{L}}_z^{(n)} \equiv -i\hbar\frac{\partial}{\partial\Phi_n}, \tag{34}$$

an *OAM* operator which acts in $(\mathcal{X}_n, \mathcal{Y}_n, \mathcal{Z})$ configuration space, upon which our physical system depends. It is easy to verify that this operator has the eigenvalue $\hbar\ell$, i.e. $\hat{\mathcal{L}}_z^{(n)}\Psi_\ell^{(n)} = \hbar\ell\Psi_\ell^{(n)}$. Whereas, as mentioned above, the states (5) and (23) are the eigenstates of $\hat{\ell}_z$ with the same eigenvalue $\hbar\ell$, i.e. $\hat{\ell}_z\psi_\ell = \hbar\ell\psi_\ell$ and $\hat{\ell}_z\Psi_\ell^{(||)} = \hbar\ell\Psi_\ell^{(||)}$, respectively. In addition, as one may expect the operator (34) coincides with the operator $\hat{\ell}_z$ when the field is switched off, $\hat{\mathcal{L}}_z^{(n)} \to \hat{\ell}_z$, (see also Eq. (35)).

To get a deeper insight let us now calculate the mean value of the conventional OAM operator averaged over the modes $\Psi_\ell^{(n)}$. For this purpose, we express $\hat{\ell}_z$ in terms of coordinates (29) by employing the relations (31)

$$\begin{aligned} \hat{\ell}_z &= -i\hbar\frac{\partial}{\partial\varphi} = -i\hbar\left(\frac{\partial\Phi_n}{\partial\varphi}\frac{\partial}{\partial\Phi_n} + \frac{\partial\Xi_n}{\partial\varphi}\frac{\partial}{\partial\Xi_n}\right) \\ &= -i\hbar\left[\frac{\partial}{\partial\Phi_n} + \mathcal{C}_n v_{\perp 0} kt\frac{\cos(\Phi_n - \phi_L)}{\Xi_n}\frac{\partial}{\partial\Phi_n}\right. \\ &\quad \left. + \mathcal{C}_n v_{\perp 0} kt\sin(\Phi_n - \phi_L)\frac{\partial}{\partial\Xi_n}\right]. \end{aligned} \tag{35}$$

Let us note that a similar operator has been derived in reference [53] to describe the electron with non-zero OAM in the presence of a strong laser field. Furthermore, for the (quantum mechanical) mean value of $\hat{\ell}_z$, when normalized to the overall "energy" of the mode (33), we obtain

$$\langle\hat{\ell}_z\rangle = \frac{\int d\boldsymbol{R}_n \left(\Psi_\ell^{(n)}\right)^* \left(\hat{\ell}_z\Psi_\ell^{(n)}\right)}{\int d\boldsymbol{R}_n \left|\Psi_\ell^{(n)}\right|^2} = \hbar\ell, \tag{36}$$

where $d\boldsymbol{R}_n = \Xi_n d\Xi_n d\Phi_n d\mathcal{Z}$ is the elementary cylindrical volume in configuration space which is related to the elementary volume in position space via $d\boldsymbol{r} = (\hbar/p_{\perp 0})^3 d\boldsymbol{R}_n$. The last two terms of the operator (35) do not contribute to the integral after the integration over $\Phi_n$. As seen, the mean values of both OAM operators coincide, $\langle\hat{\mathcal{L}}_z^{(n)}\rangle = \langle\hat{\ell}_z\rangle$. This means that, apart from the diffraction-free propagation along $z$-axis, the state (32) describes a superposition of four modes (33) each of which carries a non-zero OAM with respect to the same axis. Moreover, the time-dependent profile of the beam reveals a non-trivial dependency on the transverse coordinate $\xi$ and the azimuthal angle $\varphi$. In the next subsection, we examine this non-triviality in details and spatiotemporally characterize the Bessel beams of two-level hydrogen and selected alkali-metal atoms that are resonantly driven by the laser field without the level damping.

## 4 Spatial and temporal characterization of atomic Bessel beams

So far we have built the twisted states (23) and (30), (32) of laser-driven two-level atoms for collinear- and crossed-beam scenarios. These states can be used in order to study the space- and time-dependent profile of atomic beams.

In this section, therefore, we put the emphasis on the crossed-beam scenario and investigate how the radial distribution and the time evolution of the probability density are affected by the atomic beam velocity and the nuclear charge $Z$ when the laser field is resonant to the atomic transition energy.

To proceed with our further discussion, we define the probability density of atoms in a twisted state with a non-zero OAM $\hbar\ell$ as

$$\rho_\ell = |\Psi_\ell|^2, \tag{37}$$

such that $\rho = 1$ for beams (18) and (20) of *non-twisted* atoms. Depending on which of the two scenarios occurs, the probability density (37) acquires different forms. To show this, we substitute the wave function (23) into equation (37) and obtain the probability density for the collinear-beam scenario

$$\rho_\ell^{(\parallel)} = J_\ell^2(\xi), \tag{38}$$

as a function of only the dimensionless transverse coordinate $\xi$. Figure 2 shows the 'non-diffracting' distribution of this probability density that coincides with the beam profile of free twisted atoms (even if the laser field is still switched on). This coincidence is due to the $\xi$-independent laser phase (10) as also pointed out in Section 3.2.1.

Let us now calculate the probability density in crossed-beam scenario. For this purpose, by inserting the state (30) into equation (37), after straightforward derivations, we obtain

$$\rho_\ell^{(\perp)} = \varrho_\ell + \Delta_\ell, \tag{39}$$

where the (space- and time-dependent) term

$$\varrho_\ell = \frac{1}{4}\sum_{n=1}^{4} J_\ell^2(\Xi_n) \tag{40}$$

is responsible for the Bessel-squared-type distribution of the probability density, and the term

$$\begin{aligned}\Delta_\ell = {} & \frac{1}{2}\cos\left(\frac{\Omega_{R_z}}{\omega}\zeta_\perp + \ell(\Phi_2 - \Phi_1)\right) J_\ell(\Xi_1) J_\ell(\Xi_2) \\ & - \frac{1}{2}\cos\left(\frac{\Omega_{R_z}}{\omega}\zeta_\perp + \ell(\Phi_4 - \Phi_3)\right) J_\ell(\Xi_3) J_\ell(\Xi_4),\end{aligned} \tag{41}$$

is a small summand that can be neglected with high accuracy under properly tuned parameters of the "atom + laser" system, as shown below.

In order to explore and exhibit the temporal and spatial characteristics of atomic Bessel beams let us consider, for example, two-level hydrogen, lithium, sodium and potassium, and assume that these atoms are driven on the $1s \leftrightarrow 2p$, $2s \leftrightarrow 2p$, $3s \leftrightarrow 3p$ and $4s \leftrightarrow 4p$ atomic transitions, respectively. For the sake of simplicity, however, we here also suppose that *no* decay occurs for upper levels and, thus, that no damping applies in the time-evolution of the probability amplitudes (A.18)–(A.19). For the $1s \leftrightarrow 2p$ transition, the laser and Rabi frequencies for hydrogen can be easily expressed as

$$\omega = \frac{3e^2}{8a_0\hbar}, \quad \Omega_{R_x} = \frac{2^7 a_0 e\varepsilon_0}{3^5\hbar}, \quad \Omega_{R_z} = \sqrt{2}\Omega_{R_x} \tag{42}$$

by using the well-known properties of hydrogen-like ions [54]. For alkali-metal atoms, we make use of the known values of their spectrum [55] and dipole matrix elements [56]. Moreover, we here restrict our discussion to low- and medium-$Z$ atoms since the interaction Hamiltonian (14)–(15) is valid only within the LWA, i.e. when the radiation wavelength exceeds the atomic sizes.

After we have specified the type of a laser-driven two-level atom we are ready to explore both, the spatial and temporal characteristics of atomic Bessel beams. When the laser field is switched off, i.e. for $t = 0$, both curves for collinear- and crossed-beam scenarios coincide (cf. Fig. 2). This is quite expected since in the absence of the laser radiation only a free Bessel beam propagates, as one might also expect due to the initial conditions (A.16). Once the laser is switched on, the atomic beam starts evolving in the field and changing its conventional Bessel-squared-shape. Figure 3 displays the probability density profile (i) at various dimensionless transverse coordinates ranging from 0 to 15 at given azimuthal angle $\varphi = \pi/3$ (left panel) as well as (ii) at various azimuthal angles ranging from 0 to $2\pi$ at given (two different values of) transverse coordinate $\xi = 3$ and $\xi = 5$ (right panel). In particular, results are shown for the nonparaxial atomic beam with transverse momentum $p_{\perp 0} = p_0/5$ and OAM $\hbar\ell = 2\hbar$ as well as for the field strength $\varepsilon = 4$ GV/cm and laser propagation angle $\phi_L = \pi/2$ for three different evolution times, 10, 15 and 20 fs. Moreover, Figure 4 combines both the $\xi$- and $\varphi$-dependencies and shows the *actual* profile of Bessel beams of the same atoms when they propagate 20 fs in the field.

As seen in Figure 3, the deviation of curves from each other increases the longer the atom propagates in the laser field. This deviation is caused by all four Bessel modes in equation (40) containing the arguments

$$\begin{aligned}\Xi_n &= \sqrt{\xi^2 + 2\xi\mathcal{C}_n\zeta^{(\perp)}\frac{v_{\perp 0}}{c}\cos(\phi_L - \varphi) + \left(\mathcal{C}_n\zeta^{(\perp)}\frac{v_{\perp 0}}{c}\right)^2} \\ &\approx \sqrt{\xi^2 - 2\xi\mathcal{C}_n v_{\perp 0} kt\cos(\phi_L - \varphi)}.\end{aligned} \tag{43}$$

The time factor $2\xi\mathcal{C}_n v_{\perp 0} kt\cos(\phi_L - \varphi)$, which involves both the transition energy and the atom-laser coupling strength, can lead to an *enhancement* of the second maximum of the beam profile during its evolution in the laser field. This enhancement depends crucially on how the parameters of the "atom + laser" system are tuned. For instance, when the beam of potassium is evolved in the field within 20 fs, the first two maxima become of the same order (cf. Fig. 3d1). This can be clearly seen also (i) from Figure 3d2 in the region where the red dot-dashed curves intersect for $\xi = 3$ and $\xi = 5$ and (ii) from Figure 4 especially for the azimuthal angle $\varphi \sim \pi/2$ for which the first two maxima are well separated (white areas for the potassium profile in the vertical direction). In addition,

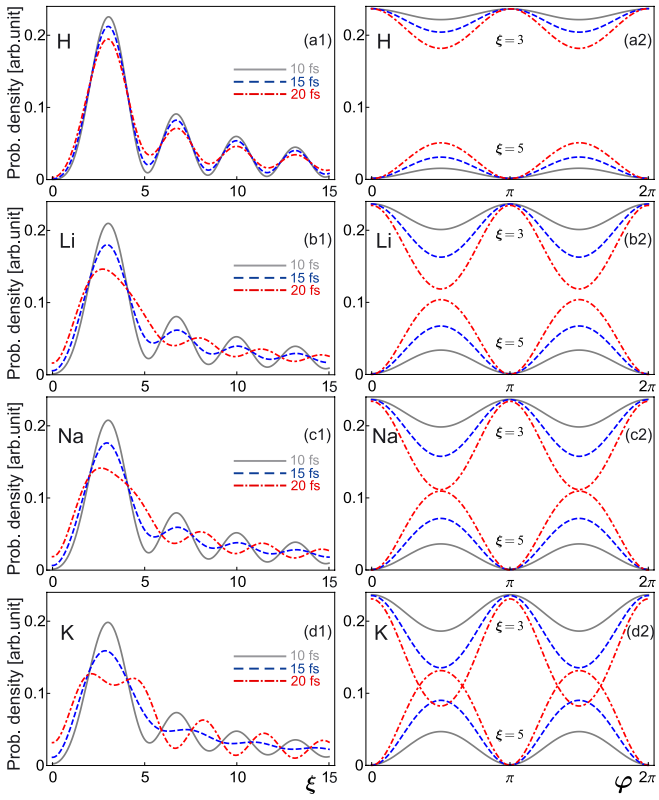


**Fig. 3.** Distribution of probability density $\rho_\ell^{(\perp)}$ (in arbitrary units) as a function of dimensionless transverse coordinate $\xi = p_{\perp 0} r/\hbar$ ((a1)–(d1)) and azimuthal angle $\varphi$ ((a2)–(d2)) for $\ell = 2$. The probability densities are shown for Bessel beams of H (a1-2) with atomic velocity $1.4 \times 10^6$ cm/s and of Li (b1-2), Na (c1-2), K (d1-2) with atomic velocity $0.7 \times 10^6$ cm/s for different propagation times 10 fs (gray solid curves), 15 fs (blue dashed curves) and 20 fs (red dot-dashed curves).

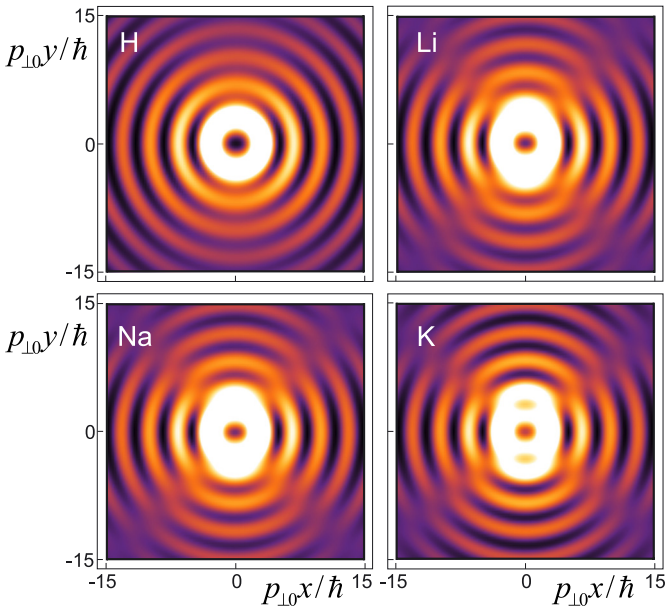


**Fig. 4.** "Snapshot" of atomic Bessel beam profiles at $t = 20$ fs after the laser, which drives the atom, is activated. The laser wave propagates along the positive direction of $y$-axis, the polarization vector points toward the observer. The parameters of the "atom + laser" system and the variation of colors are the same as in Figures 3 and 2, respectively.

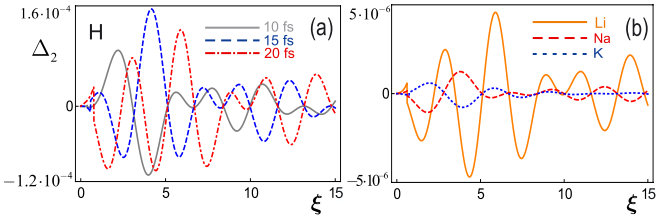


**Fig. 5.** Distribution of $\Delta_\ell$ for $\ell = 2$ as a function of dimensionless transverse coordinate $\xi = p_{\perp 0} r/\hbar$ for hydrogen with different propagation times (a) and for alkali-metal atoms with an evolution time 10 fs (b).

the probability density (40) for exact $\varphi = \pi/2$ is discussed in reference [29].

Figure 3 exhibits also another intriguing feature of the beam profile in the crossed-beam scenario (which, in fact, eventually leads to the enhancement of the second maximum). Since the term $\mathcal{C}_n v_{\perp 0} kt$ reveals different values for different atoms, this $Z$-dependency gives rise to a *field-induced 'spread'* of the Bessel-squared-shape of the atomic probability density (cf. Figs. 3b1–3d1). This behavior is rather universal and remains the same for all $z$, i.e. along the atom propagation axis. Indeed, as the nuclear charge increases the white areas in Figure 4 start to symmetrically spread along and against the propagation direction of the field, meanwhile keeping their shape constant along the $z$-axis. All these non-trivial spatiotemporal characteristics are caused by the coherent interaction of atomic and laser beams and are quantitatively reflected both in the $Z$-dependent atomic transition energy and the atom-field interaction strength, i.e. the Rabi frequency. In addition, we would like to note that the term $\Delta_\ell$ does not contribute in the radial distribution of the probability density because it is effectively zero for an evolution time varying in $0, \ldots 100$ fs and for low- and medium-$Z$ atoms (cf. Fig. 5).

As, for example, in the case of optical [57,58] and electron [58] Bessel beams, we have spatially and temporally characterized the atomic Bessel beams that are driven by the laser field. In contrast to these studies, radiation-assisted atomic beams, that carry non-zero OAM, acquire a special type of behavior, as illustrated in Figures 3–5, due to the coherent coupling of an atom to the laser field. To study these properties of the laser-driven Bessel beams experimentally, we hope that similar methods as for the creation of electron vortex beams via *nanofabricated fork-like hologram* (cf. Refs. [26–28]) will be be developed for the atomic systems. Moreover, for neutral atoms, that barely interact with the matter, we believe that this can be achieved by means of (i) atomic microscopes which deliver resolution of the order of few nm and (ii) laser systems which provide a resolution of the order of 10 fs.

## 5 Summary and conclusions

The twisted states of laser-driven two-level atoms have been built and investigated, especially, in crossed-beam scenario when the laser and atomic beams are perpendicular to each other. In more detail, the interaction of a two-level atom with a linearly polarized electromagnetic field has been described by using the space- and time-dependent laser phase for solving the Schrödinger equation in a similar way as known from relativistic quantum theory of electron. Exact analytical solution to the Schrödinger equation was found within the eikonal, rotating-wave and long-wave approximations (to deal with fields nearly resonant to the two-level excitation energy and with wavelengths larger than the atomic size). Our treatment enables one to construct a twisted state of laser-driven two-level atoms with their well defined energy, transverse and longitudinal momentum components as well as the projection of the orbital angular momentum along the propagation direction. By making use of these states, detailed calculations have been performed for the distribution of the probability density of hydrogen, lithium, sodium and potassium for the $1s \leftrightarrow 2p$, $2s \leftrightarrow 2p$, $3s \leftrightarrow 3p$ and $4s \leftrightarrow 4p$ atomic transitions, respectively, *without* (level) damping. For the crossed-beam scenario, we have exhibited a non-trivial, Bessel-squared-type behavior of the beam profile that applies for both, paraxial and nonparaxial regimes and depends on time. We have also shown that a possible enhancement of the second maximum of probability density may occur under a specific choice of laser and atom parameters, such as the atom evolution time, nuclear charge, atomic velocity, the laser frequency and the electric field strength.

Though emphasis was placed on the interaction of two-level atoms with external (monochromatic) fields, the theory in this work is applicable also for three- and multi-level atoms of different configurations, including $\Lambda$-, $V$- and $\Sigma$-type atoms. Moreover, this theory can be extended quite easily to a (general) elliptically polarized monochromatic field as well as to a *standing* wave $\boldsymbol{E} = (\varepsilon\cos(\boldsymbol{k}\cdot\boldsymbol{r}-\omega t)+\varepsilon\cos(\boldsymbol{k}\cdot\boldsymbol{r}+\omega t), 0, 0)$. The latter case will enable one, for instance, to deal also with *elastic* interactions between the atom and the field. In the future, moreover, it seems desirable to us (and possible) to construct a unitary operator of the form

$$U_\ell^{(\shortparallel)}(t,t') = \frac{\cos(\Omega_0^{(\shortparallel)}\zeta^{(\shortparallel)}/2)}{\cos(\Omega_0^{(\shortparallel)}\zeta'^{(\shortparallel)}/2)}\, e^{i\alpha_0^{(\shortparallel)}\omega(t-t')}\ |a\rangle\langle a| + \frac{\sin(\Omega_0^{(\shortparallel)}\zeta^{(\shortparallel)}/2)}{\sin(\Omega_0^{(\shortparallel)}\zeta'^{(\shortparallel)}/2)}\, e^{i\beta_0^{(\shortparallel)}\omega(t-t')}\ |b\rangle\langle b|$$

with the phase $\zeta'^{(\shortparallel)} \equiv k_{||}z-\omega t'$ at some initial state in the collinear-beam scenario, in order to describe collision and scattering phenomena with atomic Bessel beams. Such evolution operators would be useful also for investigation of form factors of Bessel beams of radiation-assisted two-level systems, such as molecules, atoms or even nuclei [59].

A.G.H. thanks Dr. Marco Ornigotti and Dr. Filippo Fratini for useful comments and acknowledges the support from the GSI Helmholtzzentrum and the University of Heidelberg. O.M. and A.S. acknowledge support from the Helmholtz Gemeinschaft and GSI (Nachwuchsgruppe VH-NG-421).

## Appendix: Derivation of solutions of the Schrödinger equation

To determine the probability amplitudes $\psi_a$ and $\psi_b$ for the atomic states $|a\rangle$ and $|b\rangle$, we take into account that the overall dynamics of the atom-laser system remains the same for the collinear- and crossed-beam scenarios (compare Eqs. (14)–(15)), though they imply different coupling strengths and phases in the interaction Hamiltonian. For these similar Hamiltonians, in our further calculations we will adopt generic notations $\Omega_R$, $\phi_d$ and $\zeta$ in order to replace the Rabi frequencies $\Omega_{R_x}$, $\Omega_{R_z}$, the dipole matrix element exponentials $\phi_{d_x}$, $\phi_{d_z}$ and the laser phases $\zeta_{||}$, $\zeta_\perp$, respectively. The replacement of these laser phases is justified since the solution which we construct does not depend on any preferred direction of the laser wave vector.

In order to describe the dynamics of laser-driven two-level atoms we take into account that the laser phase $\zeta$ contains both, the time- and space-variables and, therefore, enables one to express the corresponding partial deri-vatives by the total derivative with regard to this phase. Based on this mathematical trick we can re-write the Schrödinger equation as an ordinary differential equation in a similar way as the Dirac equation has been examined earlier by Volkov [30] and Skobelev [60,61] who found solutions for the (relativistic) motion of electrons and neutrons, respectively. Thus, by making use of this technique and substituting ansatz (17) into the time-dependent Schrödinger equation (16), we obtain the two coupled equations

$$\frac{\hbar^2k^2}{2m}\psi_a'' + i\hbar\,(\boldsymbol{v}\cdot\boldsymbol{k}-\omega)\,\psi_a' - E_a\psi_a + \hbar\Omega_R e^{-i\phi_d}\cos\zeta\psi_b = 0$$

$$\frac{\hbar^2k^2}{2m}\psi_b'' + i\hbar\,(\boldsymbol{v}\cdot\boldsymbol{k}-\omega)\,\psi_b' - + E_b\psi_b + \hbar\Omega_R e^{i\phi_d}\cos\zeta\psi_a = 0,$$

where the prime refers to a derivation with regard to the phase $\zeta$ and $\boldsymbol{v} = \boldsymbol{p}/m$ denotes the center-of-mass velocity of the atom with the non-relativistic energy $\mathcal{E} = p^2/(2m)$. Similar techniques have been applied more recently also to the Mott scattering of an electron in the presence of intense single-mode laser fields [62], both within the relativistic and non-relativistic regimes. For non-relativistic electrons and neutrons, moreover, such an approach was taken in references [63] and [64,65], respectively.

Owing to the (large) mass $m$ of the atom, whose rest energy $mc^2$ is much larger than the photon energy $\hbar\omega$, we typically have $\hbar^2k^2/(2m\hbar\omega) \leq 10^{-10}$ even for ultraviolet frequencies and can hence make use of the EA [66]. In this approximation, we will drop the first terms in the last system of equations and rewrite them in the form

$$\psi_a' + i\alpha\psi_a = i\Omega\, e^{-i\phi_d}\,\cos\zeta\,\psi_b, \tag{A.1}$$

$$\psi_b' + i\beta\psi_b = i\Omega\, e^{i\phi_d}\,\cos\zeta\,\psi_a, \tag{A.2}$$

by introducing the following notations

$$\alpha \equiv \frac{E_a}{\hbar\left(\boldsymbol{v}\boldsymbol{k}-\omega\right)},\, \beta \equiv \frac{E_b}{\hbar\left(\boldsymbol{v}\boldsymbol{k}-\omega\right)},\, \Omega \equiv \frac{\Omega_R}{\boldsymbol{v}\boldsymbol{k}-\omega}. \quad \text{(A.3)}$$

The denominator $\boldsymbol{v}\cdot\boldsymbol{k}-\omega$ hereby illustrates the Doppler shifted radiation frequency as seen by the moving atom [66].

Equations (A.1) and (A.2) describe the evolution of the probability amplitudes in EA. To find solutions for these two first-order equations, we may use the ansatz

$$\psi_a = A(\zeta)\, e^{-i\alpha\zeta}, \quad \text{(A.4)}$$

$$\psi_b = B(\zeta)\, e^{-i\beta\zeta} \quad \text{(A.5)}$$

to bring them into the simpler form

$$A' = i\Omega\, e^{-i\phi_d}\, \cos\zeta\, e^{i(\alpha-\beta)\zeta}\, B, \quad \text{(A.6)}$$

$$B' = i\Omega\, e^{i\phi_d}\, \cos\zeta\, e^{-i(\alpha-\beta)\zeta}\, A, \quad \text{(A.7)}$$

in which the second terms on the left-hand side of equations (A.1) and (A.2) have been eliminated. As we will see below, this re-definition (A.4) and (A.5) of the probability amplitudes facilitates the integration of equations (A.6)–(A.7). In addition, we could also *decouple* these two equations by taking the second derivative with regard to the phase $\zeta$,

$$A'' + (-i(\alpha-\beta)+\tan\zeta)\, A' + \Omega^2\cos^2\zeta\, A = 0 \quad \text{(A.8)}$$

$$B'' + (i(\alpha-\beta)+\tan\zeta)\, B' + \Omega^2\cos^2\zeta\, B = 0, \quad \text{(A.9)}$$

and for which solutions are known in terms of hypergeometric functions [33]. However, in this work we are interested in laser frequencies which are nearly resonant to atomic transition frequency. Therefore, we apply RWA to obtain solutions to equations (A.8) and (A.9) in terms of elementary functions.

In our further discussion, as usual, we consider frequencies (of the radiation field) which are in resonance with or nearly resonant to the atomic excitation, $\hbar\omega \approx E_a - E_b$. In such a *resonance* regime, it is justified to apply the RWA for which the exact solutions can be found for equations (A.6) and (A.7). If the counter-rotating terms proportional to $\exp\left[\pm i\left(\alpha-\beta-1\right)\zeta\right]$ are ignored on the right-hand side, these equations take the form

$$A' = \frac{i\Omega}{2} e^{-i\phi_d} e^{i(\alpha-\beta+1)\zeta}\, B, \quad \text{(A.10)}$$

$$B' = \frac{i\Omega}{2} e^{i\phi_d} e^{-i(\alpha-\beta+1)\zeta}\, A. \quad \text{(A.11)}$$

An (exact) solution for $A$ and $B$ is then given by

$$\left(\mu_1-\mu_2\right) A\left(\zeta\right) = -\left[A(0)\mu_2 - \frac{i\Omega}{2} e^{-i\phi_d} B(0)\right] e^{\mu_1\zeta} + \left[A(0)\mu_1 - \frac{i\Omega}{2} e^{-i\phi_d} B(0)\right] e^{\mu_2\zeta}, \quad \text{(A.12)}$$

$$\left(\mu_1-\mu_2\right) B\left(\zeta\right) = \left[B(0)\mu_1 + \frac{i\Omega}{2} e^{i\phi_d} A(0)\right] e^{-\mu_2\zeta} - \left[B(0)\mu_2 + \frac{i\Omega}{2} e^{i\phi_d} A(0)\right] e^{-\mu_1\zeta}, \quad \text{(A.13)}$$

with

$$\mu_{1,2} = \frac{i}{2}\left(\alpha-\beta+1\pm\delta\right), \quad \text{(A.14)}$$

$$\delta \equiv \sqrt{\left(\alpha-\beta+1\right)^2+\Omega^2}, \quad \text{(A.15)}$$

and where $A\left(0\right)$ and $B\left(0\right)$ refer to "initial" conditions with regard to the laser phase, $\zeta = 0$. These initial conditions are fulfilled, for instance, at the origin $\boldsymbol{r} = 0$, $t = 0$ of the space and time coordinates. Owing to the existence of the phase $\zeta$, however, the solutions (A.12) and (A.13) are more general and can be analyzed in order to explore the time- and space-dependency of the probability amplitudes explicitly, if one wishes to take into account the wave vector of the laser field and the motion of the atom as a whole. For the atom at rest ($\boldsymbol{p} = 0$) and if we also ignore the $\boldsymbol{k}$-dependence of the laser beam, i.e. simply perform a replacement $\zeta \to -\omega t$, the solutions (A.12) and (A.13) simplify to

$$A\left(t\right) = \left\{A(0)\left[\cos\frac{\Lambda_2 t}{2} - i\frac{\Lambda_1}{\Lambda_2}\sin\frac{\Lambda_2 t}{2}\right] + i\frac{\Omega_R}{\Lambda_2}\, e^{-i\phi_d}\, B(0)\sin\frac{\Lambda_2 t}{2}\right\} e^{i\frac{\Lambda_1 t}{2}},$$

$$B\left(t\right) = \left\{B(0)\left[\cos\frac{\Lambda_2 t}{2} + i\frac{\Lambda_1}{\Lambda_2}\sin\frac{\Lambda_2 t}{2}\right] + i\frac{\Omega_R}{\Lambda_2}\, e^{i\phi_d}\, B(0)\sin\frac{\Lambda_2 t}{2}\right\} e^{-i\frac{\Lambda_1 t}{2}}$$

with $\hbar\Lambda_1 = E_a - E_b - \hbar\omega$ and $\Lambda_2^2 = \Lambda_1^2 + \Omega_R^2$, and are in full agreement with standard texts on the two-level atom [34]. Using equations (A.12) and (A.13), moreover, the conservation of the overall probability of the atom, namely of being in one of the two states, $\left|\psi_a\right|^2 + \left|\psi_b\right|^2 = 1$, can be verified quite easily.

Although an oscillation of the probability amplitudes $\psi_a$ and $\psi_b$ can be seen already from ansatz (A.4)–(A.5), further insights are obtained if we specify the "initial" conditions for these probability amplitudes and modulate the field in a resonance regime with the atomic transition frequencies. Therefore, two remarks are in order here before we shall further examine the solutions (A.12)–(A.13)

for the amplitudes $A(\zeta)$ and $B(\zeta)$. First, the initial condition for $\zeta = 0$ should be chosen properly. If we assume the atom initially to be in the upper state, we have

$$A\,(0) = 1, \qquad B\,(0) \;=\; 0, \tag{A.16}$$

for the interaction of the atom with linearly polarized field [34]. Second, we still have some freedom in general of how to choose the physical parameters, such as the momentum $\boldsymbol{p}$ of the atom, its energies $E_a, E_b$ of the upper and lower states, the frequency $\omega$ of the coupling field as well as the Rabi frequency $\Omega_R$. Apart from a suitable choice of the two-level atom, these parameters are often controlled by the intensity and the propagation direction of the external field(s) acting upon the atom. For example, we may readily fulfill the *resonance* condition by assuming a field with frequency $\omega$, so that

$$E_a - E_b = \hbar\omega_{\,\mathrm{eff}} \;\equiv\; \hbar\omega\,\Big(1 + \frac{\boldsymbol{v}\cdot\boldsymbol{n}}{c}\Big),$$

and where $\boldsymbol{n}$ is the unit vector along the propagation direction of the field as used before. This resonance condition gives rise to the simple relation

$$\alpha - \beta + 1 = 0 \tag{A.17}$$

for the reduced quantities (A.3).

If we substitute the initial condition (A.16) into the solutions (A.12)–(A.13) for a linearly polarized field, the *phase*-dependent probability amplitudes read as

$$A = \frac{i\mu_2}{\delta}\, e^{\mu_1\zeta} - \frac{i\mu_1}{\delta}\, e^{\mu_2\zeta},$$

$$B = \frac{\Omega}{2\delta}\, e^{i\phi_d} e^{-\mu_2\zeta} - \frac{\Omega}{2\delta} e^{i\phi_d}\, e^{-\mu_1\zeta},$$

and, together with the resonance condition (A.17), take the simple form

$$A = \cos\frac{\Omega\zeta}{2}, \tag{A.18}$$

$$B = ie^{i\phi_d}\sin\frac{\Omega\zeta}{2}, \tag{A.19}$$

where we have used the relations (A.14)–(A.15). Hence, if we use the ansatz (17) and equations (A.4)–(A.5) and then recover the corresponding expressions of generic notations $\Omega_R$, $\phi_d$ and $\zeta$, we will arrive to the form (18) and (20) for the laser-driven two-level atom in collinear- and crossed-beam scenario, respectively.

To summarize this derivation, we have found exact solutions (A.18)–(A.19) for a particular coupling of the atomic motion to the radiation field by applying the eikonal, long-wave and rotating-wave approximations. In practice, these three approximations are well justified if the frequency of the electric field is nearly resonant to the two-level excitation energy (for the RWA), the laser wavelength is larger than the atomic sizes (for the LWA) and since the de Broglie wavelength of an atom is typically much smaller than the wavelength of the radiation field (for the EA). Of course, the RWA might fail if the resonance condition is not fulfilled to a sufficient degree which may lead to the standard Bloch shift [67] or some generalized Bloch-Siegert shift [68].

## References


1. J. Durnin, J. Opt. Soc. Am. **4**, 651 (1987)
2. J. Durnin, J.J. Miceli Jr., J.H. Eberly, Phys. Rev. Lett. **58**, 1499 (1987)
3. D. McGloin, K. Dholakia, Contemp. Phys. **46**, 15 (2005)
4. R. Jáuregui, S. Hacyan, Phys. Rev. A **71**, 033411 (2005)
5. S.K. Tiwari, S.R. Mishra, S.P. Ram, H.S. Rawat, Appl. Opt. **51**, 3718 (2012)
6. Y. Ismail, N. Khilo, V. Belyj, A. Forbes, J. Opt. **14**, 085703 (2012)
7. L. Allen, S.M. Barnett, M.J. Padgett, *Optical Angular Momentum* (Institute of Physics Publishing, Bristol and Philadelphia, 2003)
8. J.P. Torres, L. Torner, *Twisted Photons: Applications of Light with Orbital Angular Momentum* (Wiley-VCH Verlag GmbH & Co. KGaA, Weinheim, 2011)
9. L. Allen, M.W. Beijersbergen, R.J.C. Spreeuw, J.P. Woerdman, Phys. Rev. A **45**, 8185 (1992)
10. J. Arlt, V. Garcés-Cháves, W. Sibbert, K. Dholakia, Opt. Commun. **197**, 239 (2001)
11. D.G. Grier, Nature **424**, 810 (2003)
12. M.E.J. Friese, J. Enger, H. Rubinsztein-Dunlop, N.R. Heckenberg, Phys. Rev. A **54**, 1593 (1996)
13. J. Arlt, K. Dholakia, Opt. Commun. **177**, 297 (2000)
14. S. Schmid, G. Thalhammer, K. Winkler, F. Lang, J.H. Denschlag, New J. Phys. **8**, 159 (2006)
15. M. Liu, T. Zentgraf, Y. Liu, G. Bartal, X. Zhang, Nat. Nanotechnol. **5**, 570 (2010)
16. J.W.R. Tabosa, D.V. Petrov, Phys. Rev. Lett. **83**, 4967 (1999)
17. V. Garcés-Cháves, D. McGloin, M.J. Padgett, W. Dultz, H. Schmitzer, K. Dholakia, Phys. Rev. Lett. **91**, 093602 (2003)
18. M. Merano, N. Hermosa, J.P. Woerdman, A. Aiello, Phys. Rev. A **82**, 023817 (2010)
19. A. Aiello, New J. Phys. **14**, 013058 (2012)
20. A. Mair, A. Vaziri, G. Weihs, A. Zeilinger, Nature **412**, 313 (2001)
21. M.F. Andersen, C. Ryu, P. Cladé, V. Natarajan, A. Vaziri, K. Helmerson, W.D. Phillips, Phys. Rev. Lett. **97**, 170406 (2006)
22. S. Franke-Arnold, L. Allen, M. Padgett, Laser Photon. Rev. **2**, 299 (2008)
23. K.Y. Bliokh, Y.P. Bliokh, S. Savel'ev, F. Nori, Phys. Rev. Lett. **99**, 190404 (2007)
24. K.Y. Bliokh, M.R. Dennis, F. Nori, Phys. Rev. Lett. **107**, 174802 (2011)
25. M. Uchida, A. Tonomura, Nature **464**, 737 (2010)
26. J. Verbeeck, H. Tian, P. Schattschneider, Nature **467**, 301 (2010)
27. J. Verbeeck, P. Schattschneider, S. Lazar, M. Stöger-Pollach, S. Löffler, A. Steiger-Thirsfeld, G. Van Tendeloo, Appl. Phys. Lett. **99**, 203109 (2011)
28. B.J. McMorran, A. Agrawal, I.M. Anderson, A.A. Herzing, H.J. Lezec, J.J. McClelland, J. Unguris, Science **331**, 192 (2011)
29. A.G. Hayrapetyan, S. Fritzsche, Phys. Scr. T., accepted
30. V.B. Berestetskii, E.M. Lifshitz, L.P. Pitaevskii, *Quantum Electrodynamics* (Pergamon Press, Oxford, 1982)
31. U.D. Jentschura, V.G. Serbo, Phys. Rev. Lett. **106**, 013001 (2011)

32. U.D. Jentschura, V.G. Serbo, Eur. Phys. J. C **71**, 1571 (2011)
33. I.S. Gradshtein, I.M. Ryzhik, *Table of Integrals, Series and Products* (Academic Press, 2000)
34. M.O. Scully, M.S. Zubairy, *Quantum Optics* (Cambridge University Press, 2001)
35. L. Allen, J. Eberly, *Optical Resonance and Two-Level Atoms* (Dover Publications, 1987)
36. C.J. Foot, *Atomic Physics* (Oxford University Press, 2005)
37. C. Cohen-Tannoudji, D. Guéry-Odelin, *Advances in Atomic Physics: An overview* (World Scientific, 2011)
38. V.V. Kozlov, Y. Rostovtsev, M.O. Scully, Phys. Rev. A **74**, 063829 (2006)
39. C. Champenois, G. Hagel, M. Houssin, M. Knoop, C. Zumsteg, F. Vedel, Phys. Rev. Lett. **99**, 013001 (2007)
40. D.A. Cardimona, P.M. Alsing, H. Mozer, C. Rhodes, Phys. Rev. A **79**, 063817 (2009)
41. L.-M. Duan, A. Sørensen, J.I. Cirac, P. Zoller, Phys. Rev. Lett. **85**, 3991 (2000)
42. H.-R. Noh, W. Jhe, J. Opt. Soc. Am. B **27**, 1712 (2010)
43. P. Kumar, A.K. Sarma, Phys. Rev. A **84**, 043402 (2011)
44. G. Andrelczyk, M. Brewczyk, Ł. Dobrek, M. Gajda, M. Lewenstein, Phys. Rev. A **64**, 043601 (2001)
45. L.E. Helseth, Phys. Rev. A **69**, 015601 (2004)
46. X.-J. Liu, H. Jing, X. Liu, M.-L. Ge, Eur. Phys. J. D **37**, 261 (2006)
47. J.D. Jackson, *Classical Electrodynamics* (John Wiley & Sons, 2001)
48. I.I. Rabi, Phys. Rev. **51**, 652 (1937)
49. K.J. Meharg, J.S. Parker, K.T. Taylor, J. Phys. B **38**, 237 (2005)
50. G.J. Zeng, Phys. Rev. A **63**, 053408 (2001)
51. P. Schattschneider, J. Verbeeck, Ultramicroscopy **111**, 1461 (2011)
52. K.Y. Bliokh, M.A. Alonso, E.A. Ostrovskaya, A. Aiello, Phys. Rev. A **82**, 063825 (2010)
53. D.V. Karlovets, Phys. Rev. A **86**, 062102 (2012)
54. B.H. Bransden, C.J. Joachain, *Physics of Atoms and Molecules* (Longman, London and New York, 1983)
55. R.G. Parsons, V.F. Weisskopf, Z. Phys. **202**, 492 (1967)
56. H.J. Metcalf, P. van der Straten, *Laser Cooling and Trapping* (Springer, New York, Berlin, 1999)
57. K.B. Kuntz, B. Braverman, S.H. Youn, M. Lobino, E.M. Pessina, A.I. Lvovsky, Phys. Rev. A **79**, 043802 (2009)
58. K.Y. Bliokh, F. Nori, Phys. Rev. A **86**, 033824 (2012)
59. B. Povh, K. Rith, C. Scholz, F. Zetsche, *Particles and Nuclei* (Springer, 2008)
60. V.V. Skobelev, Sov. Phys. J. Exp. Theor. Phys. **67**, 1322 (1988)
61. V.V. Skobelev, Sov. Phys. J. Exp. Theor. Phys. **68**, 221 (1989)
62. C. Szymanowski, V. Véniard, R. Taïeb, A. Maquet, C.H. Keitel, Phys. Rev. A **56**, 3846 (1997)
63. A.R. Mkrtchyan, R.M. Avakyan, A.G. Hayrapetyan, B.V. Khachatryan, R.G. Petrosyan, Armenian J. Phys. **2**, 258 (2009)
64. A.R. Mkrtchyan, A.G. Hayrapetyan, B.V. Khachatryan, R.G. Petrosyan, Phys. At. Nucl. **73**, 478 (2010)
65. K.K. Grigoryan, A.G. Hayrapetyan, R.G. Petrosyan, Nucl. Instrum. Methods B **268**, 2539 (2010)
66. L.D. Landau, E.M. Lifshitz, *Theoretical Physics: The Classical Theory of Fields* (Butterworth-Heineman, 2000), Vol. 2
67. F. Bloch, A. Siegert, Phys. Rev. **57**, 522 (1940)
68. J. Tuorila, M. Silveri, M. Sillanpää, E. Huneberg, Y. Makhlin, P. Hakonen, Phys. Rev. Lett. **105**, 257003 (2010)